Design and synthesis of aliphatic supramolecular polymers featuring amide, urethane, and urea hydrogen bonding units

Tareq, A. Z., Hyder, M., Hermida Merino, D., Mohan, S. D. ORCID: https://orcid.org/0000-0001-5388-088X, Cooper, J. A. ORCID: https://orcid.org/0000-0002-3981-9246 and Hayes, W. ORCID: https://orcid.org/0000-0003-0047-2991 (2025) Design and synthesis of aliphatic supramolecular polymers featuring amide, urethane, and urea hydrogen bonding units. European Polymer Journal, 228. 113782. ISSN 1873-1945 doi: 10.1016/j.eurpolymj.2025.113782 Available at https://centaur.reading.ac.uk/120491/

European Polymer Journal 228 (2025) 113782

Contents lists available at ScienceDirect

European Polymer Journal

journal homepage: www.elsevier.com/locate/europolj

Design and synthesis of aliphatic supramolecular polymers featuring amide, urethane, and urea hydrogen bonding units

Alarqam Zyaad Tareq [a], Matthew Hyder [a], Daniel Hermida Merino [b], Saeed D. Mohan [c], James.A. Cooper [a], Wayne Hayes [a,*]

[a] Department of Chemistry, University of Reading, Whiteknights, Reading RG6 6AD, UK
[b] DUBBLE CRG, BM26, ESRF-The European Synchrotron, Netherlands Organization for Scientific Research, 6 rue Jules Horowitz, 38043 Grenoble, France
[c] Centre for Advanced Microscopy, Chemical Analysis Facility, University of Reading, Whiteknights, Reading RG6 6ED, UK

ARTICLE INFO

Keywords:
Supramolecular polyurethane
Phase separation
Hydrogen bonds
Amide units

ABSTRACT

Functionalisation of polyurethane-urea oligomers with hydrogen bonding amide end groups leads to dramatic thermal, mechanical, morphological, and rheological changes of supramolecular polyurethane elastomers. This study reports the design, synthesis and characterisation of six new aliphatic thermally stable supramolecular polyurethanes (SPUs). It was found that introduction of the amide end groups affords a polymer network that is maintained by dynamic associations within the solid state of the material. Through atomic force microscopy (AFM), the aggregation of hard segments of these phase separated SPU networks was found to be more prominent with the introduction of the amide end groups. The strong hydrogen bonding associations between the amide end groups were complemented by urea-urea and urethane-urethane interactions from the main chains to enhance the self-assembly and phase separation of SPUs and also improve the mechanical, thermal and rheological properties with respect to other SPU elastomers that feature bisamide end groups. These thermally stable phase separated SPUs also displayed remarkable re-adhesive capabilities on both glass and aluminium substrates, for example, **SPU2** exhibited unique reusability after seven adhesion cycles.

1. Introduction

Supramolecular polymer networks formed via hydrogen bonding interactions between the polymer chains have been shown to exhibit remarkable characteristics corresponding to their intrinsically dynamic properties. [1–4] This dynamic nature provides the polymers with the high selectivity and tuneable properties via the reversible association and dissociation of the hydrogen bonds present within the networks. [5–7]

Many fundamental synthetic studies have produced numerous elegant hydrogen bonded assemblies. [8,9] Lehn and co-workers reported supramolecular liquid crystalline polymers through association of three hydrogen bonds between 2,6-diaminopyridine with 2,6-diamino-1,3,5-trizine (bifunctional chiral), tartaric acid (as a spacer), and uracil derivatives (as side-chains). [10] A notable and extensively studied hydrogen bonding recognition motif in supramolecular polymers is the 2-ureido-4[1H]-pyrimidinone (UPy) system, first reported by Meijer and co-workers in 1997 that assembles via the formation of quadruple hydrogen bonds. [11–16] Guan and co-workers reported novel thermoplastic elastomers combining of polystyrene hard segments (backbone) and polyacrylate amide (side chains) soft segments. The hydrogen-bonding brush motifs enable the polymer to heal up to 92 % in terms of extension to break relative to the pristine material at 25 °C. [17].

Polyurethanes (PUs) are used extensively in modern society on account of the low cost of the raw materials and the desirable physical properties of these materials. [18] Applications of PUs are diverse and include coatings, [19] fibers, [20] foams, [21] 3D and 4D printing, [22–24] and the biomedical field. [25–27] Novel healable polyurethanes have been reported by Liu and co-workers via inserting dynamic covalent chains that enhanced the mechanical and thermal properties (T_g was increased from 23 °C to 80 °C), as well as the healing efficiency.[28] The effect of hard segment content in polyurethanes has been investigated by Wilkes and co-workers – different aliphatic and aromatic diisocyanates were assessed and revealed that the symmetry of the diisocyanate was crucial to the degree of hydrogen bonding and

* Corresponding author.
E-mail address: w.c.hayes@reading.ac.uk (W. Hayes).

https://doi.org/10.1016/j.eurpolymj.2025.113782
Received 19 November 2024; Received in revised form 22 January 2025; Accepted 28 January 2025
Available online 31 January 2025

microphase separation that in turn influenced the thermal properties and dynamic mechanical behaviour. [29] In a subsequent study, segmented supramolecular polyurethanes formed using two different diisocyanates (4,4′–methylenediphenyl diisocyanate (4,4′-MDI) and 1,6-hexamethylene diisocyanate (HDI) with triptycene units as a chain extender – the materials generated with HDI exhibited enhanced microphase separation in comparison to those derived from MDI on account of the flexibility of HDI segments. [30].

Amide units can also promote self-assembly of supramolecular polymer networks via the self-complementary interactions of the carbonyl acceptor groups and amine donors groups. [31–34] Chang and co-workers have successfully generated supramolecular polyamide-urethane blends with $LiClO_4$ to produce dynamic electrolyte materials in which the phase separation within the bulk phase was enhanced via strong associations of the amide groups. [35] Leibler and co-workers have reported telechelic supramolecular polymers based on polypropylene oxide functionalised with thymine and diaminotriazine end groups. [36] These polymers exhibited self-healing properties via reformation of hydrogen bonds between the thymine and diaminotriazine units. In addition, the hydrogen bonding interaction between amide groups in thymine motifs improved the microphase segregation and crystallization behaviour of the final polymers. [36].

In previous studies, we have reported several telechelic SPU systems that exhibited self-assembling and healable properties across a range of temperatures. [22,27,37,38] In common with the findings of other groups, [39,40] the combination of phase separation in these supramolecular polymer networks and hydrogen bonding afforded enhanced thermal and mechanical properties in comparison to the parent polymers. [41–44] Herein, we report a series of novel aliphatic SPUs derived from a telechelic polymer (hydrogenated poly(butadiene) and HDI that are terminated with several different aliphatic amide end-group units. This investigation enabled the effect the hydrogen-bonding motifs of the aliphatic amide end-group have on the viscoelastic properties to be determined. Four amino aliphatic end-groups featuring amide functionalities were designed and synthesised to assess their ability to reinforce the phase separation and assembly of SPUs. It was found that the strong association of these end-groups developed the thermal, rheological, and mechanical characteristics of the SPU networks whilst also enabling these materials the ability to recover their properties post-damage.

2. Experimental

2.1. Materials

Krasol™ HLBH-P 2000 (molecular weight as supplied = 2100 g/mol) was kindly provided by Total Cray Valley, all other reagents used were purchased from Sigma Aldrich, TCI, Acros Organics, Fisher Chemical and Fluorochem. The solvents THF and $CHCl_3$ were dried by using an MBRAUN SP7 system fitted with activated alumina columns. The synthesis and characterisation data of the compounds and polymers described in this paper are reported in the Supporting Information (SI) file.

2.2. Characterisation

^{1}H NMR and ^{13}C NMR spectra were measured using either a Bruker Nanobay 400 or a Bruker DPX 400 spectrometer operating for ^{1}H NMR (400 MHz) or ^{13}C NMR (100 MHz) spectroscopic analysis. Chemical shifts (δ) are reported in ppm relative to $CDCl_3$ (δ 7.26 ppm) and the residual solvent resonance (δ 2.50 ppm) for DMSO-d_6, (δ 1.94) CD_3CN, and (δ 1.73 ppm) THF-d_8 in ^{1}H NMR spectra. Fourier-Transform Infrared (FT-IR) spectroscopic analysis was carried out at room temperature using a Perkin Elmer 100 FT-IR instrument equipped with a diamond-ATR sampling accessory. Variable-temperature IR (VT-IR) spectroscopic analysis was carried out over the temperature range 20——220 °C (via a heating–cooling cycle) using a Perkin Elmer 100 FT-IR spectrometer with a Specac variable-temperature cell holder and Temperature Controller. Sample was analysed as a potassium-bromide disc with a material loading of 1 % wt. The temperature was measured locally with a thermocouple embedded inside the solid-cell frame. The resulting spectra were analysed using the Perkin Elmer spectrum IR software (version 10.6.2). Mass spectrometry (MS) was conducted using a Thermo Fisher Scientific Orbitrap XL LCMS. The sample was introduced by liquid chromatography (LC) and sample ionisation achieved by electrospray ionization (ESI). The average molecular weights of the polymers generated were determined via Gel Permeation Chromatography (GPC) using an Agilent Technologies 1260 Infinity I system in HPLC-grade THF at a flow rate of 1.0 mL min^{-1}. Calibration was achieved using a series of near monodisperse polystyrene standards and samples were prepared at a concentration of 1.0 mg mL^{-1}. Differential calorimetry (DSC) measurements were performed on a TA Instruments X3 DSC adapted with a TA Refrigerated Cooling System (RCS90), using aluminium TA Tzero pans and Hermetic lids, measuring from −80 °C to 200 °C with heating and cooling rates of 5 °C min^{-1} under nitrogen gas with a flow rate of 50 mL min^{-1}. Thermogravimetric analysis (TGA) was carried out on TA Instruments TGA Q50 instrument with aluminium Tzero pans. The sample was heated from 20 °C to 600 °C at 10 °C min^{-1} under nitrogen gas with a flow rate of 60 mL min^{-1}. Thermal characterisation of samples was investigated using the TRIOS software (version 5.1.1). Rheological measurements were performed on a Malvern Panalytical Kinexus Lab + instrument fitted with a Peltier plate cartridge and 8 mm parallel plate geometry and analysed using rSpace Kinexus v1.76.2398 software. Tensile tests were carried out using a Thümler Z3-X1200 tensometer at a rate of 10 mm min^{-1} with a 1 kN load cell and analysed using THSSD-2019 software. Optical microscopy videos were captured using a Leica DM1000 microscope equipped with a Mettler Toledo FP82 hot stage. The sample was placed onto a glass slide and then placed into the hot stage chamber, the temperature of which is controlled by an FP90 Central Processor (heating rate 10 °C min^{-1}). All videos were recorded using Studio86Designs software. Small-angle X-ray scattering (SAXS) and Wide-angle X-ray scattering (WAXS) experiments were performed on a Bruker Nanostar instrument. Samples were mounted in modified DSC pans equipped with Kapton™ windows and mounted in an MRI electrical heating unit for temperature control. The atomic force microscopy (AFM) was conducted in the Centre for Advance Microscopy (CfAM) at the University of Reading using the Cypher S AFM (Oxford Instruments-Asylum Research, Santa Barbara, USA). The AFM stage movement within the x ,y and z directions were controlled using piezoelectric stacks. The scans were recorded through the user interface, Igor Pro (Version 16.33.234), using the standard Alternating Contact (AC) Topography mode (tapping mode) operating in air using a silicon tip with a resonant frequency set at approximately 70 kHz and a spring constant of approximately 2.0 Nm^{-1} (AC240TS-R3, Oxford Instruments). Each sample was dropped cast onto a 10 mm diameter AFM mica disc, first cleaved with Sellotape. Each disc was mounted onto 15 mm diameter magnetic stainless steel AFM specimen discs using 9 mm diameter carbon adhesive tabs and secured onto the microscope scanner stage magnetically. Then, through the user interface, the objective focus was adjusted and set to focus on the tip and on each sample in turn. The cantilever was autotuned at its resonance which automatically determined the drive amplitude and drive frequency. The resolution, scan rate, integral gain and scan size were entered into the user interface before starting the scan. The software Gwyddion (version 2.63) was used for data analysis and editing.

3. Results and Discussion

3.1. End-group design.

In order to demonstrate the self-assembly and phase separation of the aliphatic SPUs via hydrogen bonding, multifunctional hydrogen

bonding aliphatic amide end-groups were designed and synthesised (see Fig. 1).[45] The synthetic protocols used to afford these end-groups and the associated characterisation data are provided in the Supporting Information (SI) file (see **Figs. S1-S18**).

4. End-group self-assembly

The self-assembling end-groups of the polyurethane chains were assessed via ^{1}H NMR spectroscopy, to ascertain the end-group dimerization constant (K_D)[46–48], this was achieved using model end-group analogues,[49,50] for structural, synthetic, and spectroscopic data see the SI file. An initial ^{1}H NMR titration was conducted between two different derivatives (heterodimer) of the model end-groups (1:1) at various concentrations between 1 and 0.1 mmol, with spectra being collected from solutions-compositions of end-group derivatives in chloroform to ascertain the dimerization constant.[13] The chemical shifts of the N–H urea and amide protons are dependent on the concentrations; as the concentration decreased upon dilution with $CDCl_3$, the singlet resonances shift upfield indicating the dissociation of the hydrogen bonds, see **Table S1** and **Fig. S19-S42.**[51] K_D can be observed for these hetro-model derivatives which assume dimerization (Table 1), where K_D increases through the series i.e. from **4** to **5** to **6**. This trend in increasing K_D is attributed to the introduction of subsequent amide groups to these molecules.[52] The same pattern was observed for derivatives **1** to **2**, where K_D increased after introduction of a single amide to the end-groups. It was not possible to determine the dimerization constant of **3** from NMR dilution experiments, as a result of precipitation upon cooling post dissolution. It is worth noting that the dimerisation constant values presented here are still significantly lower than that reported for quadruple hydrogen bonding systems reported by Meijer [12] and Zimmerman [53], where the dimerisation constants reported were as high as $> 10^{6}$ M^{-1} and 10^{7} M^{-1}, respectively.

4.1. Synthesis of supramolecular polyurethanes

A library of novel SPUs (**SPU1-SPU6**) have been synthesised via a one-pot, two-step route [37,43,54] as summarised in Scheme 1. Firstly, hydrogenated poly(butadiene) (Krasol HLBH-P 2000) (1.00 equiv.) was dried at 80 °C under reduced pressure for 3 h. Hexamethylene diisocyanate (HDI) (2.05 equiv.) and catalyst (dibutyltin dilaurate (DBTDL (0.5 wt% of reactants)) were then added to the dried polymeric diol. After reacting for 3 h at 80 °C in the bulk under argon atmosphere, the desired isocyanate terminated polyurethane pre-polymer (NCO:OH ratio of 2.05:1) was generated. The pre-polymer was then solvated in anhydrous THF or $CHCl_3$ and the amine-functionalised end groups (2.05 equiv.) were then added. The mixture was stirred for 18 h at 60 °C to obtain the desired aliphatic SPU (83 % – 90 %). Each reaction was monitored via FTIR spectroscopy, until the isocyanate absorbance band at 2272–2248 cm^{-1} was not evident, a period of *ca.* 18 h was typically required. The SPUs were isolated after several precipitations into ice-cold methanol.

To confirm the successful synthesis of the aliphatic SPUs, ^{1}H NMR, ^{13}C NMR, and FTIR spectroscopic analysis were employed, see **Fig. S43-S60**. FTIR spectra of the SPUs revealed key absorbance bands at 1708–1716 cm^{-1}, 1684–1698 cm^{-1}, and 1635–1643 cm^{-1} corresponding to the carbonyl stretches of the urethanes, urea, and amide functional groups, respectively. Furthermore, ^{1}H NMR spectroscopic analysis revealed key resonances at *ca.* 7.30 ppm, 6.15 ppm, and 5.32 ppm, which were attributed to the protons of the amide and urea units of the multifunctional end-group derivatives and the urethane units derived from the pre-polymer, respectively. In addition, ^{13}C NMR spectroscopy was used to confirm the formation of the urethane, urea and amide linkages in the aliphatic SPUs with key resonances observed at *ca.* 157.5 ppm, 158.5 ppm, and 172.5 ppm, respectively. The appearance of the cast SPUs films varied from clear to opaque as a result of phase separation aided via hydrogen bonding interactions of the amide end groups, see **Fig. S61**. GPC analysis of the SPUs confirmed an average degree of chain extension of 3–5, (see Table 2 and **Fig. S62**) consistent with the synthesis of structurally-related SPUs.[27,43,45] The high M_w and high dispersity (Đ) values observed were attributed to the aggregation of the polymer chains arising from the strong intermolecular associations within the solutions tested.[45,55].

DSC and TGA analyses were used to examine the thermal characteristics of the SPUs, as shown in Table 3 and **Figs. S63-S74**. The highest processing temperature of SPUs was assessed via TGA by heating the polymer samples from 20 to 550 °C at a rate of 10 °C min^{-1} under a nitrogen atmosphere. The TGA plots of the SPUs revealed high thermostability for these materials and significant degradation did not occur until *ca.* 270 °C and full degradation was only observed when the temperature exceeded 475 °C and the temperature corresponding to 5 wt% loss is shown in Table 3. The endothermic events of glass transition (T_g) and melt transition (T_m), and exothermic effect of crystallisation (T_c) temperatures were examined via DSC by heating the SPUs samples from –80 to 200 °C at a rate of 5 °C min^{-1} under a nitrogen atmosphere. The DSC thermograms for the SPUs revealed a T_g at *ca.* −46.8 °C in the first heating cycle, which corresponds to the T_g of the soft segment of the amorphous hydrogenated poly(butadiene)[22,37,41] within the microphase separated polymer, see Table 4.

Melt transitions were not evident in the DSC thermogram of **SPU1** in the first and second cycles. During the first heating cycle, **SPU2** which contains one amide group and ethyl-morpholine moiety in the end-group, displayed one broad melt transitions (T_m) at *ca.* 74.5 °C corresponding to the melting hard domains of the polymer. **SPU3** has two melt transitions at 180.5 °C and 191.1 °C in the first heating cycle attributed to the dissociation of the strongly associated end-groups between the polymer chains as a result of the two amide groups. Additionally, a strong exothermic event was noticed in the first cooling cycle at 147.6 °C corresponding to cold crystallization. **SPU4** does not possess an amide group in the end-group, and exhibits a broad melt transitions at *ca.* 41.4 °C which was attributed to re-association/dissociation of the thermo-reversible crosslinking between the chains in the polymer.[56] **SPU5** exhibits a melting transition at *ca.* 81.5 °C during the first cycle which corresponds to the relaxation of the ordered hard and soft segments. Another intense melt transition was observed at *ca.* 180.0 °C during the first and second heating cycles which was attributed to the melting of hard segments in the polymer. An endothermic transition at *ca.* 127.9 °C was observed in the first heating cycle of **SPU6**, corresponding to the relaxation of the highly ordered of hard and soft segments. Additionally, during the first heating cycle, a strong melting transition was observed at *ca.* 230.6 °C with enthalpy 21.7 J/g that

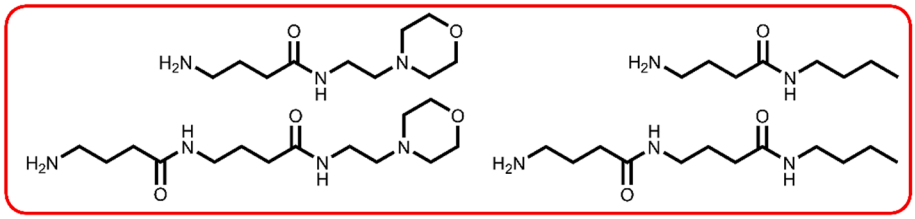

Fig. 1. The chemical structure of the end-groups.

Table 1
Dimerization constants for model derivatives in $CDCl_3$ at 25 °C.

Derivatives	Chemical structure	K_D (M^{-1})	Derivatives	Chemical structure	K_D (M^{-1})
1	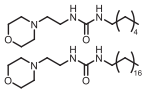	16.42 ± 3.45	**4**	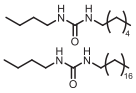	0.18 ± 0.66
2	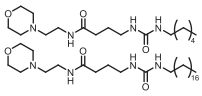	939.46 ± 5.77	**5**	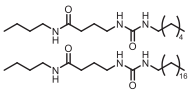	49.11 ± 3.24
3[a]	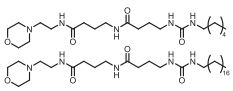	–	**6**	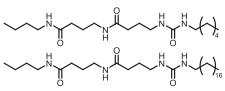	66.56 ± 3.51

[a] Dimerisation constant could not be determined.

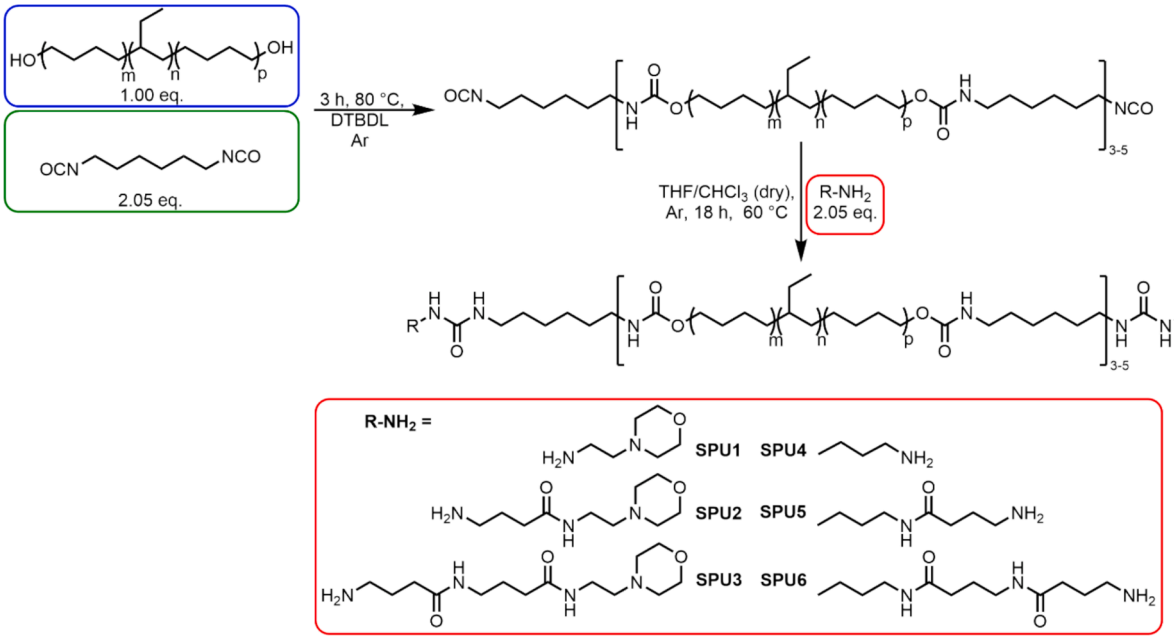

Scheme 1. The synthetic route used to generate the supramolecular polyurethanes **SPU1**–**SPU6**.

Table 2
Molecular weight of the supramolecular polymers **SPU1**–**SPU6**.

SPU (% yield)	M_n (NMR) (g/mol)	M_n (g/mol)	M_w (g/mol)	$Đ$
SPU1 (90 %)	8780	9300	15,500	1.65
SPU2 (84 %)	9450	10,000	17,400	1.73
SPU3 (86 %)	17,100	10,800	35,400	3.27
SPU4 (89 %)	8160	11,900	20,800	1.73
SPU5 (87 %)	13,160	11,000	31,900	2.89
SPU6 (83 %)	10,980	12,190	29,000	2.64

Table 3
Thermal properties of the supramolecular polymers **SPU1**–**SPU6**.

SPU	T_d 5 % (°C)	T_g (°C)[b]	T_m (°C)[a]	Enthalpy (J/g)	T_m (°C)[b]	T_{cc}[a] /T_c[c] (°C)
SPU1	299.9	−46.8	–		–	–
SPU2	295.0	−46.8	74. 5	2.2	–	–
SPU3	300.1	−46.8	180.5	1.9	–	147.6[a]
			190.1	0.6		
SPU4	306.6	−46.8	41.4	4.6	–	–
SPU5	273.7	−46.7	81.5	0.3	180.0	–
			180.2	2.5		
SPU6[d]	288.2	−46.8	127.9	4.4	199.1	174.8[c]
			230.6	21.7		

[a] First heating run 5 °C min^{-1}; [b] Second heating run 5 °C min^{-1}; [c] First cooling run 5 °C min^{-1}; [d] DSC temperature range of −80–250 °C.

corresponded to the dissociation of the end-groups between the polymer chains.

To understand the thermal stability and disassociated/re-associated states of the hydrogen-bonding interactions involving the urethane, urea, and amide moieties in the supramolecular network variable-temperature infrared (VT-IR) spectroscopic analysis was examined on **SPU5** from 20 °C to 220 °C and then back to 20 °C. The deconvolution of the amide, urea, and urethane carbonyl groups were monitored as a function of temperature, see Fig. 2. [57] At room temperature, the IR spectra of **SPU5** revealed two absorbance bands at *ca.* 1709 cm^{-1} and *ca.* 1735 cm^{-1} assigned to ordered and free hydrogen bonded of urethane carbonyl groups, respectively. [42,58] A strong absorbance band at *ca.* 1644 cm^{-1} was observed and related to associated carbonyl amide and urea groups. [59–61] As the temperature was increased, the frequency of the associated carbonyl urethane groups shifted systematically to *ca.* 1735 cm^{-1} corresponding to the presence of dissociated urethane moieties. Two significant new absorbance bands were also observed as the

Table 4
Effect of polymer end-groups on the mechanical properties of the SPUs; the values recorded are the averages of three separate samples for each SPU. The error shown is the standard deviation for the three repeat measurements for each sample.

SPU	UTS (MPa)	EB (ε)	YM (MPa)	MoT (MJm^{-3})
SPU2	1.43 ± 0.01	0.37 ± 0.02	40.41 ± 1.30	0.38 ± 0.07
SPU3	2.63 ± 0.10	0.80 ± 0.03	35.46 ± 1.53	1.45 ± 0.05
SPU4	0.94 ± 0.04	0.49 ± 0.01	13.68 ± 0.85	0.21 ± 0.04
SPU5	1.01 ± 0.04	0.86 ± 0.03	16.65 ± 1.10	0.75 ± 0.08
SPU6	4.31 ± 0.08	0.46 ± 0.01	37.94 ± 1.02	0.97 ± 0.06

temperature was increased, at *ca.* 1689 cm^{-1} and *ca.* 1673 cm^{-1}, which corresponded to the free and disordered carbonyl amide and urea groups as a result of the disassociation process of the hydrogen bonds. [62] A notable absorbance band was evident at *ca.* 1543 cm^{-1} and was assigned to the enhanced bending vibration of N–H groups in line with the increasing temperature. [63,64] The reverse trend was observed in the cooling cycle.

To assess the effect the amide motifs of the end-groups have on the association/dissociation of hydrogen bonds, rheological analysis was undertaken, see Fig. 3 and **Fig. S75**. As shown in Fig. 3, the storage modulus (G′) and tan delta (δ) were plotted against temperature in the regime from 0 °C to 200 °C, and it is evident that G′ of the SPUs increases in agreement with the number of amides in the end-groups. The significant increase in G′ arises as a result of increased hydrogen bonding interactions in the polymer network.

SPU1 and **SPU4** exhibited a simple relaxation at 17 °C and 46 °C in the storage modulus, respectively, owing to the dissociation of the supramolecular interactions in the polymer and revealed viscoelastic behaviour attributed to the absence of amide groups in their end-groups structures. Rheological analysis also revealed significant phase separation in the cases of **SPU2**, **SPU3**, **SPU5**, and **SPU6**. Extended rubbery properties up to 100 °C were observed and G' remained essentially constant between 10^6-10^7 Pa as a result of the strong association of the amide end-groups of **SPU5** and **SPU6**. A similar behaviour was also evident for **SPU3** and **SPU6** – these rheological profiles are analogous to structurally-related hydrogen bonded SPU materials.[65] **SPU3** exhibited a relaxation at 140 °C that was attributed to the crossover between G' and loss modulus (G'') as a result to the transition of polymer from a viscoelastic solid to a viscous liquid. While **SPU6** exhibited a relaxation in the range between 130 °C and 140 °C, owing to the melting of the hard segments and does not exhibit a crossover between (G') and (G'') until 200 °C. The phase-angle curves of **SPU5** and **SPU6** revealed significant relaxation in the regime from 91 °C to 120 °C and 120 °C to 135 °C, respectively, attributed to the melting of the hard domains in the polymer chains. The behaviour of **SPU5** and **SPU6** are a result of the amides in the end-groups, which improve the association between the polymer chains. Thus, the SPUs possessing alkyl units in the end-groups rather than ethyl-morpholine units have higher thermal stability. This trend could be attributed to more efficient self-assembly of the polymer chains with the alkyl units which could lead to enhance the microphase separation.[60,65].

Tensile stress–strain behaviour was examined in order to identify the effect of the different end-groups on the mechanical performance of the SPUs, as shown in Fig. 4 and Table 3. **SPU1** was a viscous polymer at room temperature rendering it unsuitable for tensile testing. Analysis of **SPU5** and **SPU6** revealed enhanced Young's modulus (YM), ultimate

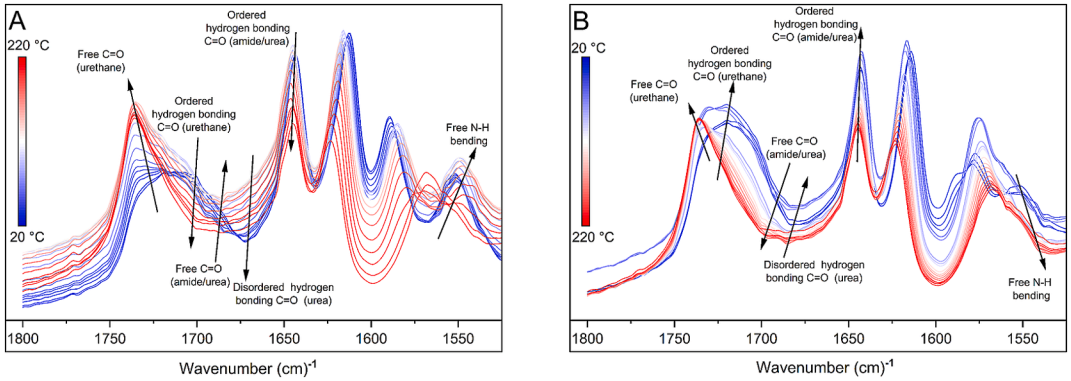

Fig. 2. VT-IR spectra of **SPU5** in the 1500 to 1800 cm^{-1} region. (**A**) Heating from 20 to 220 °C and (**B**) Cooling from 220 to 20 °C, at 10 °C intervals.

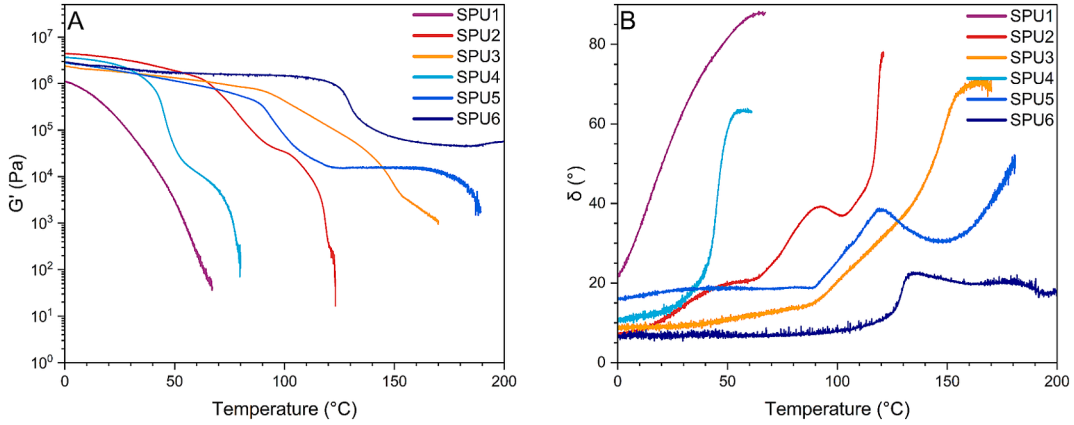

Fig. 3. The rheological behaviour of **SPU1**-**SPU6** over the temperature range of 0—200 °C, at a heating rate of 2 °C/min , using a normal force of 1 N and a frequency of 1 Hz. (**A**) storage modulus (G') against temperature, (**B**) phase angle (δ) against temperature.

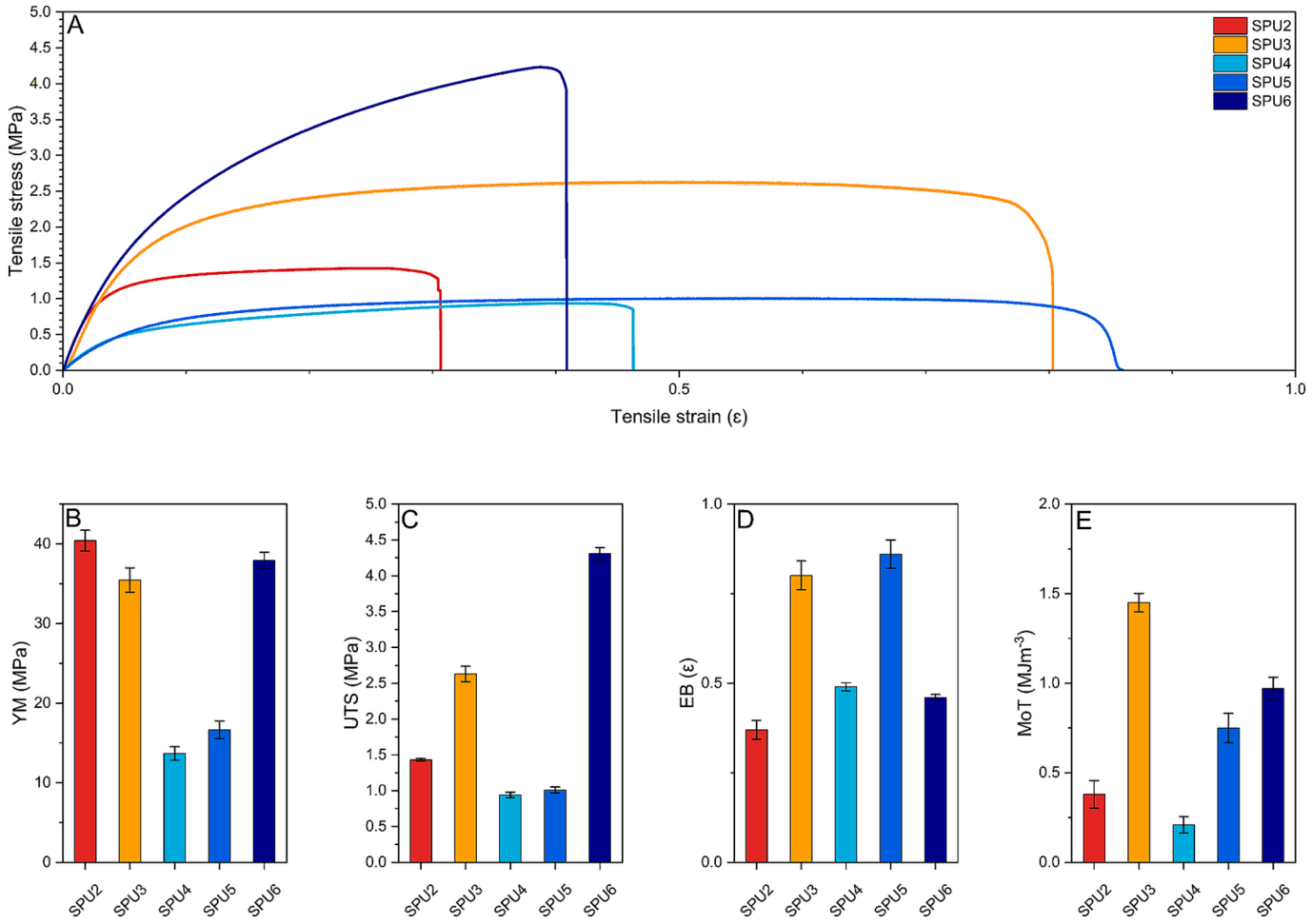

Fig. 4. Mechanical properties of **SPU2**–**SPU6**, (**A**) Tensile stress–strain curves of the SPUs, (**B**) Young's modulus (**C**) Ultimate Tensile Strength (UTS), (**D**) elongation at break (EB), and (**E**) Modulus of toughness (MoT). The error bars shown correlate to the standard deviation.

tensile strength (UTS), and modulus of toughness (MoT), compared to **SPU4**, thus confirming reinforcement of the polymer networks by the introduction of the amide units in the end-groups of these polymers. The significant increase in the resistance of polymer deformation under load (YM) for **SPU5** and **SPU6** was attributed to the amide units in the chemical structure of the end-groups of these polymers which improved the hydrogen bonded association between the polymer chains. A similar result was observed for **SPU2** and **SPU3**. The UTS, EB, and MoT values of **SPU3** (possessing two amide units in the end-groups) were considerably enhanced when compared to **SPU2**, featuring only one amide group in the end-group, as a result of the strong amide hydrogen bonds between chains in the polymer networks.

To gain further insight into the phase separation phenomena and microstructure of the supramolecular polyurethanes, the surface morphology of SPUs was assessed by atomic force microscopy (AFM) in tapping mode. Fig. 5 shows the AFM phase images of **SPU4**–**SPU6** at scan size 10 μm, 2 μm, and 500 nm, while **Figs. S76–S78** show AFM phase and height images for **SPU1**–**SPU6**. Two distinct phases were observed by the AFM analysis (phase topography) of each SPUs: the aggregation of soft segments were evident as light areas owing to the high phase angle, whereas the hard segments aggregation were visible as dark areas attributed to the low phase angle.[66–68] The phase tapping mode discloses the compositional heterogeneities of the examined polymer surfaces owing to the chemical composition of the SPUs samples.[69] All the SPUs exhibited phase separation, which became more evident with the introduction of amide groups in the end-groups. The improvement of the phase separation results from the strong association via hydrogen bonding between amide–urea and amide–amide motifs.[70] The phase images of **SPU4**–**SPU6** revealed hard domains,[71] the aggregation of these are responsible for the development of the phase separation from small portions in **SPU4** (without amide), to well-distributed sheets in **SPU5** (*ca.* 100–250 nm) with an amide group.[72] In the case of **SPU6** (with two amide groups), relatively larger sheets (*ca.* 0.3–1.2 μm) were observed that were attributed to aggregation of highly ordered hard domains.[73] Similar phase separation behaviour was also displayed in the cases of **SPU1**–**SPU3**. Additionally, the AFM height images of all SPUs confirmed the phase separation via most of the light and dark regions features. This suggests that many of the hard segment's aggregation in the phase topography images had different feature sizes on the surface of the SPUs. The topographical AFM images presented dark portions and light area in both phase and height tapping mode clearly indicated direct evidence that all of the SPUs showed phase separation that was enhanced via hydrogen bonding interactions, see Fig. 6.

The nanostructure of the SPUs probed by preliminary SAXS experiments showed a similar nanophase separation with comparable length scales to the analogous SPU derivatives.[38,43,45,65] Interestingly, a higher internal organization relating to pseudo-crystalline domains was observed in the WAXS analysis, in particular for derivatives **SPU5** and **SPU6,** with reflections at *ca.* 14.7 nm^{-1} and 16.8 nm^{-1} that are typically associated with the hydrogen bonding of urethanes and packing of the end groups, respectively.

In order to evaluate the self–healing efficiency of **SPU2**–**SPU6**, these materials were subjected to thermal stimuli by two tests. The first assay

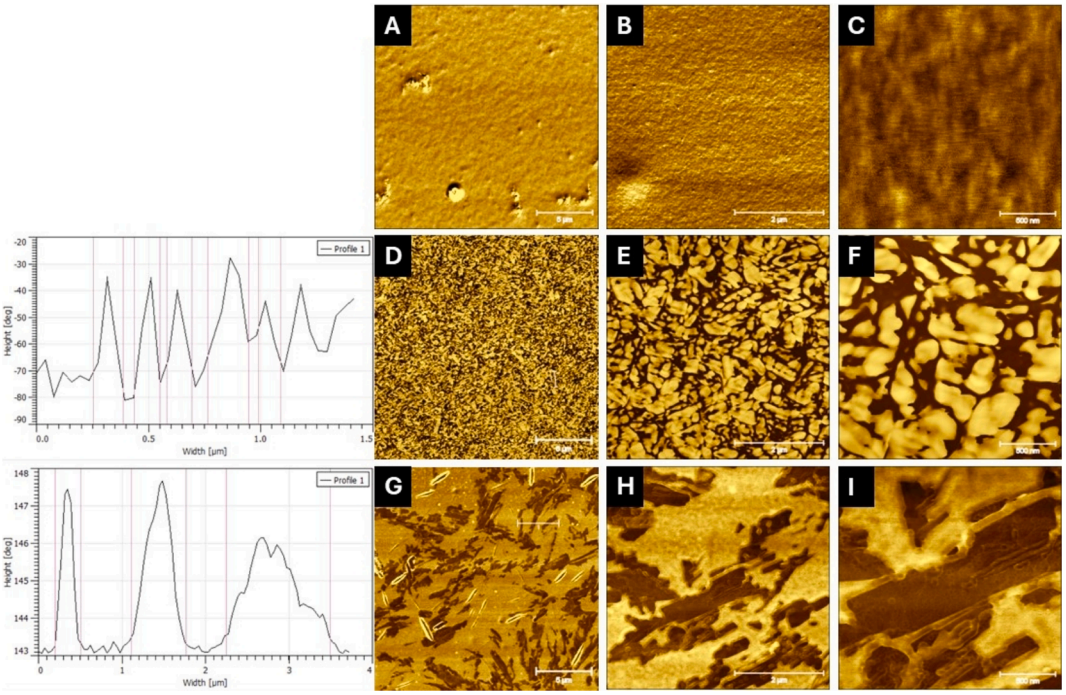

Fig. 5. AFM tapping mode phase images of **SPU4** (**A**, **B**, **C**), **SPU5** (**D**, **E**, **F**), and **SPU6** (**G**, **H**, **I**) for three different scale bars 10 µm, 2 µm, and 500 nm. All the polymer samples were prepared by drop casting from $CHCl_3$ (0.5 mg mL^{-1}) onto a mica disc.

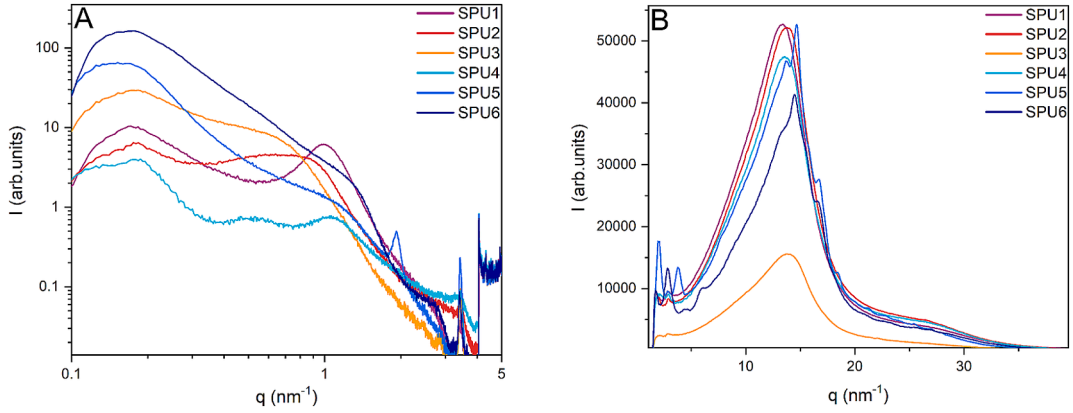

Fig. 6. (**A**) SAXS and (**B**) WAXS scattering patterns of **SPU1**-**SPU6** at 25 °C.

involved variable-temperature optical microscopy performed between 20 and 180 °C at a heating rate of 10 °C min^{-1}. In the second sets of tests, tensile strain–stress tests were conducted on healed polymer samples; **Figs. S79-S80**, **Table S2**, and Table 5 show the tensile strain–stress curves and the efficiency of healing. All the SPUs were cast as films and were cut into two parts using a scalpel blade and the healing process was studied as the temperature was increased (see **videos S2-S6** in the SI file). For tensile–stress tests, the damaged SPUs were gently re-attached on a pre-heated PTFE plate. Then the samples were placed into a pre-heated oven for two different healing times (1 and 4 h) at different temperatures (the temperature used is derived from the crossover between G' and G'' (*ca.* 10 °C below the viscoelastic transition with exception of **SPU5** and **SPU6** which were healed at 150 °C) from the rheological analysis for each polymer sample) and then cooled to room temperature for 1 h.[37,45] The variable-temperature optical microscopy of **SPU2**–**SPU6** revealed the ability of the SPUs to heal and the gap between two parts for each polymer progressively disappeared as the temperature was elevated. The damaged areas diminished in scale until the polymer films were reformed. The ability of the polymers to reform intact films as the temperature was elevated was attributed to dissociation and decreased levels of hydrogen bonding between polymer chains.[45,74] The motions of polymers chains were hindered and the free volume between these chains was contracted which thus affected on the ability to undergo efficient repair.[45,75].

Table 5
Healing efficiency of the mechanical properties of **SPU2**–**SPU6** after 1 h, calculated from pristine and healed values.

SPU	Temperature (°C)	UTS (MPa)	YM (MPa)	MoT (MJm^{-3})	EB (ε)
SPU2	100	84 %	48 %	39 %	54 %
SPU3	100	16 %	44 %	22 %	14 %
SPU4	40	39 %	50 %	68 %	88 %
SPU5	150	57 %	65 %	80 %	26 %
SPU6	150	36 %	56 %	20 %	40 %

Furthermore, tensile–stress tests of healed **SPU2**–**SPU6** revealed changes in the mechanical properties when compared to the pristine materials in terms of YM and MoT.[37,76] **SPU2** exhibited good healing behaviour: 84 % in UTS, with an EB of 54 % after 1 h. Reduced healing

efficiency was observed in the case of **SPU3** (44 % in YM and EB was decreased to 14 % after 1 h). The change observed in the ultimate tensile strength and elongation at break could be assigned to the disruption and reformation of the hydrogen bond network at the site of damage.[77] The dramatic reduction in the mechanical properties of the healed **SPU3** when compared to **SPU2** was related to the molecular characteristics of the end-groups in the supramolecular polymer network, i.e. crystallinity, hydrogen bonding, and network density, that could, in turn, affect the self-healing process of the polymer.[78,79] Modest self-healing behaviour was noticed in **SPU4** (50 % in YM and 68 % for MoT). The healing efficiency was increased after introducing amide group in the end-groups of **SPU5** when compared to **SPU4** as a result of the hydrogen bonding capability of the end groups that improved the ability of the polymer to heal. The mechanical features of the healed SPUs showed that these polymers have the ability to heal when exposed to thermal stimuli and a key trend were apparent. The healing efficiency decreased as the number of amide groups in the end-groups was increased for both SPUs bearing ethyl-morpholine and alkyl end group moieties correlated to the strength of re-association of the non-covalent interactions. Therefore, after an appropriate healing time, many of the damaged hydrogen bonding moieties may re-associate with other partner units far the damaged surfaces,[64,80] which led to reducing the number of "unbound chemical bonds" that can play a key role in self-healing processes.[7,64,80] A comparison between **SPU2** and **SPU4** to other self-healing polyurethanes[7,81–85] revealed that these SPUs exceed many in terms of UTS and EB both within their pristine and healed samples, see **Fig. S81**.

In the light of the polar urea and amide moieties and apolar polymer units in these supramolecular polyurethane polymers, these polymers had characteristics rendering them suitable for use as elastomeric adhesives. The dynamic and thermoplastic nature of the SPUs via transforming the polymeric network state from viscoelastic solid to viscoelastic liquid by heating was investigated using glass and aluminium substrates. Cast films of the SPU samples (thickness 1 mm) were cut into 0.5 cm × 0.5 cm squares and placed between two slices of either glass or aluminium slides and held by clamps from each side with an adhered polymer area of 2.5 cm × 2.5 cm. Subsequent cooling to room temperature enabled to re-association of the SPUs network between the substrates. The adhesion process was conducted at different bonding temperatures (that was held below viscoelastic transition of the polymer); 40 °C (**SPU4**), 100 °C (**SPU2** and **SPU3**), and 150 °C (**SPU5** and **SPU6**) for 30 min and then allowed to cool to room temperature for 30 min. The SPUs were then investigated for their use as reusable adhesives and to establish the effects of the amide groups and number of them in the end-groups of SPUs on the shear strength. Fig. 7**(A) and (B)** show the re-adhesion of **SPU2**–**SPU6** over three cycles and for **SPU2** the test was repeated for three further cycles to examine its extended re-adhesive capability. The shear strength of the SPUs for both substrates (glass and aluminium) was increased with the introduction of the amide groups in the end-groups of the polymers resulting from improved adhesion capability via hydrogen bonding. The shear strength of SPUs was increased gradually, **SPU6>SPU5>SPU4**, after introducing amide groups in the end-groups of the polymer and the number of amide units play an important role to enhance the adhesion properties of the polymer. In addition, **SPU2** and **SPU5** (both possessing one amide group per end group) exhibited notable retention shear strength on both glass (95 % and 91 %) and aluminium (96 % and 83 %) substrates, respectively, over 3 cycles of re-adhesion, see **Table S3 and S4**. **SPU4** (without amide groups in the end-group) displayed the lowest adhesive capability of (0.69 ± 0.04 MPa and 0.63 ± 0.07 MPa) on both glass and aluminium, respectively, as a result to absence of the amide end-group motifs in the structure when compared to **SPU5** and **SPU6**.[45].

In addition, **SPU2** presented a remarkable adhesion to glass and aluminium substrates after seven re-adhesion cycles (from 0.97 ± 0.01 MPa to 0.90 ± 0.05 MPa, and from 0.87 ± 0.02 MPa to 0.80 ± 0.01 MPa, respectively), exemplifying the reusability of supramolecular

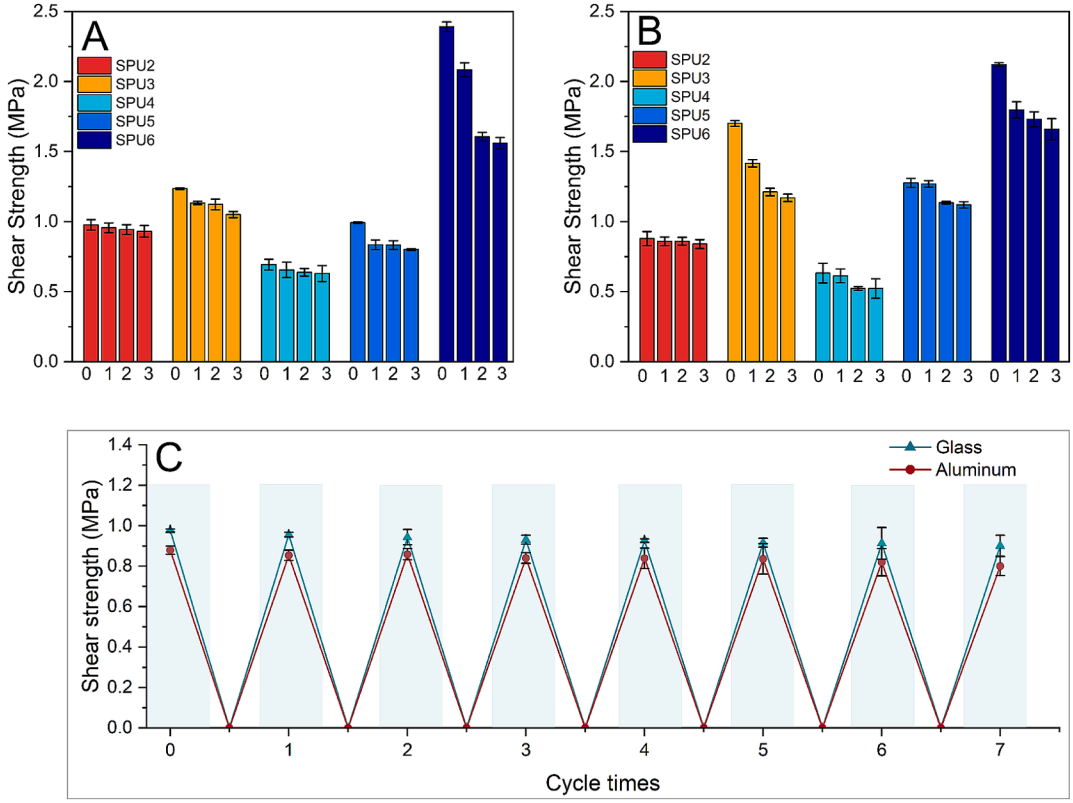

Fig. 7. Comparison of the shear strength of **SPU2**–**SPU6** over three re-adhesion cycles. Lap shear strength on (A) glass and (B) aluminum. (C) Shear strength of **SPU2** after seven cycling adhesion testing. The error bars shown correlate to the standard deviation.

polymers as adhesives, see Fig. 7 (**C**). This adhesive behaviour of **SPU2** can be attributed to dynamic nature of the assemble chains of the supramolecular polymer that enhanced the adhesive force via high-density hydrogen bonds between the carbonyl groups of the polymer and the hydrophilic surfaces of the substrates.[80,86,87].

5. Conclusions

In this paper is reported the successfully demonstrated generation of six new aliphatic supramolecular polyurethanes (SPUs) with good self-healing and adhesive capability. By increasing the hydrogen bonding interactions of the end-groups in the SPUs, via the introduction of amide units, phase separated materials were produced with improved the rheological, mechanical, and thermal properties in comparison to related SPUs. AFM images revealed the aggregation of the self-assembled hard domains, and the phase separation systematically improved via strong association of the amide groups as donor/acceptor hydrogen bonding units. Thermal analysis revealed that the melt transition of the polymer was increased with the amide groups in the end-groups. The crossover between storage modulus and loss modulus of the SPUs shifted to higher temperatures after introduction of amides into the end-groups of both ethyl-morpholine and alkyl moieties. In addition, the mechanical characterisation was also enhanced, **SPU6** displayed increased YM and UTS, by 271 % and 458 %, respectively, when compared to **SPU4**. Over three re-adhesion cycles on glass and aluminium substrates, retention of the shear strength was observed for both **SPU2** (95 % and 91 %) and **SPU5** (96 % and 83 %), respectively. Additionally, **SPU2** presented excellent reusability after seven re-adhesion cycles when tested on both glass and aluminium substrates. These SPUs also exhibit excellent healing behaviour, **SPU2** showed good healing: 84 % in UTS, with an EB of 54 % after 1 h at 100 °C.

Author Contributions

Alarqam Z. Tareq: Conceptualisation, Validation, Formal analysis, Investigation, Writing – Original Draft. **Matthew Hyder**: Conceptualisation, Formal analysis, Investigation, Visualization. **Daniel Hermida Merino**: Formal analysis & Editing. **Saeed Mohan**: Formal analysis & Editing. **James. A. Cooper**: Supervision & Editing. **Wayne Hayes**: Conceptualisation, Resources, Writing – Review & Editing, Supervision, Project administration. All authors reviewed the manuscript.

Author Statement

The authors have not made use of generative AI or AI-assisted technologies in the preparation of this manuscript and associated files.

CRediT authorship contribution statement

Alarqam Zyaad Tareq: . **Matthew Hyder:** Visualization, Investigation, Formal analysis, Conceptualization. **Daniel Hermida Merino:** Writing – review & editing, Formal analysis. **Saeed D. Mohan:** . **James. A. Cooper:** Writing – review & editing, Supervision. **Wayne Hayes:** Writing – review & editing, Supervision, Resources, Project administration, Conceptualization.

Declaration of competing interest

The authors declare that they have no known competing financial interests or personal relationships that could have appeared to influence the work reported in this paper.

Acknowledgements

The authors would like to acknowledge the financial support from HCED Iraq (PhD studentship for A.Z.T.) and from the University of Reading and Domino Printing Sciences Ltd (PhD studentship for M.H.). In addition, the University of Reading (EPSRC – Doctoral Training Grant) is acknowledged for providing access to instrumentation in the Chemical Analysis Facility. We thank Total Cray Valley for the kind supply of (hydrogenated poly(butadiene) Krasol™ HLBH-P 2000 and Mr Nick Spencer (Chemical Analysis Facility (CAF), University of Reading) for collecting the SAXS and WAXS data.

Appendix A. Supplementary data

Supplementary data to this article can be found online at https://doi.org/10.1016/j.eurpolymj.2025.113782.

Data availability

Data will be made available on request.

References

[1] Q. Wan, B.C. Thompson, Control of Properties through Hydrogen Bonding Interactions in Conjugated Polymers, Adv. Sci. 11 (2024) 2305356.
[2] M. Juanes, R.T. Saragi, W. Caminati, A. Lesarri, The Hydrogen Bond and Beyond: Perspectives for Rotational Investigations of Non-Covalent Interactions, Chem. Eur. J. 25 (49) (2019) 11402–11411.
[3] B. Tang, M. Pauls, C. Bannwarth, S. Hecht, Photoswitchable Quadruple Hydrogen-Bonding Motif, J. Am. Chem. Soc. 146 (1) (2024) 45–50.
[4] L.R. Hart, J.L. Harries, B.W. Greenland, H.M. Colquhoun, W. Hayes, Healable supramolecular polymers, Polym. Chem. 4 (18) (2013) 4860–4870.
[5] S.J.D. Lugger, S.J.A. Houben, Y. Foelen, M.G. Debije, A.P.H.J. Schenning, D. J. Mulder, Hydrogen-Bonded Supramolecular Liquid Crystal Polymers: Smart Materials with Stimuli-Responsive, Self-Healing, and Recyclable Properties, Chem. Rev. 122 (5) (2022) 4946–4975.
[6] F. Herbst, D. Döhler, P. Michael, W.H. Binder, Self-Healing Polymers via Supramolecular Forces, Macromol. Rapid Commun. 34 (3) (2013) 203–220.
[7] N. Roy, B. Bruchmann, J.-M. Lehn, DYNAMERS: dynamic polymers as self-healing materials, Chem. Soc. Rev. 44 (11) (2015) 3786–3807.
[8] G. Armstrong, M. Buggy, Hydrogen-bonded supramolecular polymers: A literature review, J Mater Sci. 40 (3) (2005) 547–559.
[9] J.H.K.K. Hirschberg, L. Brunsveld, A. Ramzi, J.A.J.M. Vekemans, R.P. Sijbesma, E. W. Meijer, Helical self-assembled polymers from cooperative stacking of hydrogen-bonded pairs, Nature 407 (6801) (2000) 167–170.
[10] T. Gulik-Krzywicki, C. Fouquey, J. Lehn, Electron microscopic study of supramolecular liquid crystalline polymers formed by molecular-recognition-directed self-assembly from complementary chiral components, Proc. Natl. Acad. Sci. 90 (1) (1993) 163–167.
[11] B.J.B. Folmer, R.P. Sijbesma, R.M. Versteegen, J.A.J. van der Rijt, E.W. Meijer, Supramolecular Polymer Materials: Chain Extension of Telechelic Polymers Using a Reactive Hydrogen-Bonding Synthon, Adv. Mater. 12 (12) (2000) 874–878.
[12] R.P. Sijbesma, F.H. Beijer, L. Brunsveld, B.J.B. Folmer, J.H.K.K. Hirschberg, R.F. M. Lange, J.K.L. Lowe, E.W. Meijer, Reversible Polymers Formed from Self-Complementary Monomers Using Quadruple Hydrogen Bonding, Science 278 (5343) (1997) 1601–1604.
[13] F.H. Beijer, R.P. Sijbesma, H. Kooijman, A.L. Spek, E.W. Meijer, Strong Dimerization of Ureidopyrimidones via Quadruple Hydrogen Bonding, J. Am. Chem. Soc. 120 (27) (1998) 6761–6769.
[14] F.H. Beijer, H. Kooijman, A.L. Spek, R.P. Sijbesma, E.W. Meijer, Self-Complementarity Achieved through Quadruple Hydrogen Bonding, Angew. Chem. Int. Ed. 37 (1–2) (1998) 75–78.
[15] J.H.K.K. Hirschberg, F.H. Beijer, H.A. van Aert, P.C.M.M. Magusin, R.P. Sijbesma, E.W. Meijer, Supramolecular Polymers from Linear Telechelic Siloxanes with Quadruple-Hydrogen-Bonded Units, Macromolecules 32 (8) (1999) 2696–2705.
[16] R.J. Wojtecki, M.A. Meador, S.J. Rowan, Using the dynamic bond to access macroscopically responsive structurally dynamic polymers, Nature Mater. 10 (1) (2011) 14–27.
[17] Y. Chen, A.M. Kushner, G.A. Williams, Z. Guan, Multiphase design of autonomic self-healing thermoplastic elastomers, Nat Chem. 4 (6) (2012) 467–472.
[18] H.-W. Engels, H.-G. Pirkl, R. Albers, R.W. Albach, J. Krause, A. Hoffmann, H. Casselmann, J. Dormish, Polyurethanes: Versatile Materials and Sustainable Problem Solvers for Today's Challenges, Angew. Chem. Int. Ed. 52 (36) (2013) 9422–9441.
[19] A.D. O'Donnell, S. Salimi, L.R. Hart, T.S. Babra, B.W. Greenland, W. Hayes, Applications of supramolecular polymer networks, React. Funct. Polym. 172 (2022) 105209.
[20] M. Sáenz-Pérez, T. Bashir, J.M. Laza, J. García-Barrasa, J.L. Vilas, M. Skrifvars, L. M. León, Novel shape-memory polyurethane fibers for textile applications, Text. Res. J. 89 (6) (2019) 1027–1037.
[21] D.T. Sheppard, K. Jin, L.S. Hamachi, W. Dean, D.J. Fortman, C.J. Ellison, W. R. Dichtel, Reprocessing Postconsumer Polyurethane Foam Using Carbamate Exchange Catalysis and Twin-Screw Extrusion, ACS Cent. Sci. 6 (6) (2020) 921–927.
[22] S. Salimi, Y. Wu, M.I.E. Barreiros, A.A. Natfji, S. Khaled, R. Wildman, L.R. Hart, F. Greco, E.A. Clark, C.J. Roberts, W. Hayes, A 3D printed drug delivery implant formed from a dynamic supramolecular polyurethane formulation, Polym. Chem. 11 (20) (2020) 3453–3464.

[23] Y. Xu, Y. Wang, H. Wei, T. Dai, Z. Li, J. Li, F. Luo, H. Tan, 4D printable shape memory polyurethane with quadruple hydrogen bonding assembly, J. Polym. Sci. 62 (14) (2024) 3258.
[24] L.R. Hart, Y. He, L. Ruiz-Cantu, Z. Zhou, D. Irvine, R. Wildman, W. Hayes, Chapter 15 - 3D and 4D printing of biomaterials and biocomposites, bioinspired composites, and related transformers, in: K.K. Sadasivuni, K. Deshmukh, M.A. Almaadeed (Eds.), 3D and 4D Printing of Polymer Nanocomposite Materials, Elsevier (2020) 467-504.
[25] S. Wendels, L. Avérous, Biobased polyurethanes for biomedical applications, Bioact. Mater. 6 (4) (2021) 1083–1106.
[26] M. Hutin, E. Burakowska-Meise, W.P.J. Appel, P.Y.W. Dankers, E.W. Meijer, From Molecular Structure to Macromolecular Organization: Keys to Design Supramolecular Biomaterials, Macromolecules 46 (21) (2013) 8528–8537.
[27] A. Feula, X. Tang, I. Giannakopoulos, A.M. Chippindale, I.W. Hamley, F. Greco, C. Paul Buckley, C.R. Siviour, W. Hayes, An adhesive elastomeric supramolecular polyurethane healable at body temperature, Chem. Sci. 7 (7) (2016) 4291–4300.
[28] L. Zhang, H. Wang, Z. Dai, Z. Zhao, F. Fu, X. Liu, The dynamic chain effect on healing performance and thermo-mechanical properties of a polyurethane network, React. Funct. Polym. 146 (2020) 104444.
[29] S. Das, D.F. Cox, G.L. Wilkes, D.B. Klinedinst, I. Yilgor, E. Yilgor, F.L. Beyer, Effect of Symmetry and H-bond Strength of Hard Segments on the Structure-Property Relationships of Segmented, Nonchain Extended Polyurethanes and Polyureas, J MACROMOL SCI B 46 (5) (2007) 853–875.
[30] Z. Chang, M. Zhang, A.G. Hudson, E.B. Orler, R.B. Moore, G.L. Wilkes, S.R. Turner, Synthesis and properties of segmented polyurethanes with triptycene units in the hard segment, Polymer 54 (26) (2013) 6910–6917.
[31] C. Cox, H. Wack, T. Lectka, Strong Hydrogen Bonding to the Amide Nitrogen Atom in an "Amide Proton Sponge": Consequences for Structure and Reactivity, Angew. Chem. Int. Ed. 38 (6) (1999) 798–800.
[32] M. Seo, J. Park, S.Y. Kim, Self-assembly driven by an aromatic primary amide motif, Org. Biomol. Chem. 10 (28) (2012) 5332–5342.
[33] C.B. Aakeröy, B.M.T. Scott, J. Desper, How robust is the hydrogen-bonded amide 'ladder' motif, New J. Chem. 31 (12) (2007) 2044–2051.
[34] L. Song, T. Zhu, L. Yuan, J. Zhou, Y. Zhang, Z. Wang, C. Tang, Ultra-strong long-chain polyamide elastomers with programmable supramolecular interactions and oriented crystalline microstructures, Nat Commun. 10 (1) (2019) 1315.
[35] Y.-C. Yen, C.-C. Cheng, S.-W. Kuo, F.-C. Chang, A New Poly(amide urethane) Solid State Electrolyte Containing Supramolecular Structure, Macromolecules 43 (5) (2010) 2634–2637.
[36] J. Cortese, C. Soulié-Ziakovic, S. Tencé-Girault, L. Leibler, Suppression of Mesoscopic Order by Complementary Interactions in Supramolecular Polymers, J. Am. Chem. Soc. 134 (8) (2012) 3671–3674.
[37] M. Hyder, A.D. O'Donnell, A.M. Chippindale, I.M. German, J.L. Harries, O. Shebanova, I.W. Hamley, W. Hayes, Tailoring viscoelastic properties of dynamic supramolecular poly(butadiene)-based elastomers, Mater. Today Chem. 26 (2022) 101008.
[38] D.H. Merino, A.T. Slark, H.M. Colquhoun, W. Hayes, I.W. Hamley, Thermo-responsive microphase separated supramolecular polyurethanes, Polym. Chem. 1 (8) (2010) 1263–1271.
[39] J. Xu, P. Chen, J. Wu, P. Hu, Y. Fu, W. Jiang, J. Fu, Notch-Insensitive, Ultrastretchable, Efficient Self-Healing Supramolecular Polymers Constructed from Multiphase Active Hydrogen Bonds for Electronic Applications, Chem. Mater. 31 (19) (2019) 7951–7961.
[40] W.P.J. Appel, G. Portale, E. Wisse, P.Y.W. Dankers, E.W. Meijer, Aggregation of Ureido-Pyrimidinone Supramolecular Thermoplastic Elastomers into Nanofibers: A Kinetic Analysis, Macromolecules 44 (17) (2011) 6776–6784.
[41] S. Salimi, L.R. Hart, A. Feula, D. Hermida-Merino, A.B.R. Touré, E.A. Kabova, L. Ruiz-Cantu, D.J. Irvine, R. Wildman, K. Shankland, W. Hayes, Property enhancement of healable supramolecular polyurethanes, Eur. Polym. J. 118 (2019) 88–96.
[42] D. Hermida-Merino, B. O'Driscoll, L.R. Hart, P.J. Harris, H.M. Colquhoun, A. T. Slark, C. Prisacariu, I.W. Hamley, W. Hayes, Enhancement of microphase ordering and mechanical properties of supramolecular hydrogen-bonded polyurethane networks, Polym. Chem. 9 (24) (2018) 3406–3414.
[43] D. Hermida Merino, A. Feula, K. Melia, A.T. Slark, I. Giannakopoulos, C.R. Siviour, C.P. Buckley, B.W. Greenland, D. Liu, Y. Gan, P.J. Harris, A.M. Chippindale, I. W. Hamley, W. Hayes, A systematic study of the effect of the hard end-group composition on the microphase separation, thermal and mechanical properties of supramolecular polyurethanes, Polymer 107 (2016) 368–378.
[44] D. Hermida-Merino, G.E. Newby, I.W. Hamley, W. Hayes, A. Slark, Microphase separation induced in the melt of Pluronic copolymers by blending with a hydrogen bonding urea–urethane end-capped supramolecular polymer, Soft Matter 11 (29) (2015) 5799–5803.
[45] A.Z. Tareq, M. Hyder, D.H. Merino, A.M. Chippindale, A. Kaur, J.A. Cooper, W. Hayes, Thermally and mechanically robust self-healing supramolecular polyurethanes featuring aliphatic amide end caps, Polymer 302 (2024) 127052.
[46] H.K.S. Tan, Determination of the NMR monomer shift and dimerization constant in a self-associating system by direct application of the least-squares method, J. Chem. Soc., Faraday Trans. 90 (23) (1994) 3521–3525.
[47] C. Jenn-shing, F. Rosenberger, Accurate nmr data evaluation for monomer shift, dimer shift and dimerization constant in a self-associating system, Tetrahedron Lett. 31 (28) (1990) 3975–3978.
[48] P. Thordarson, Determining association constants from titration experiments in supramolecular chemistry, Chem. Soc. Rev. 40 (3) (2011) 1305–1323.
[49] F. Lortie, S. Boileau, L. Bouteiller, N,N′-Disubstituted Ureas: Influence of Substituents on the Formation of Supramolecular Polymers, Chem. Eur. J. 9 (13) (2003) 3008–3014.
[50] N.E. Botterhuis, S. Karthikeyan, A.J.H. Spiering, R.P. Sijbesma, Self-Sorting of Guests and Hard Blocks in Bisurea-Based Thermoplastic Elastomers, Macromolecules 43 (2) (2010) 745–751.
[51] S.H.M. Söntjens, R.P. Sijbesma, M.H.P. van Genderen, E.W. Meijer, Stability and Lifetime of Quadruply Hydrogen Bonded 2-Ureido-4[1H]-pyrimidinone Dimers, J. Am. Chem. Soc. 122 (31) (2000) 7487–7493.
[52] W.E. Vallejo Narváez, E.I. Jiménez, E. Romero-Montalvo, A. Sauza-de la Vega, B. Quiroz-García, M. Hernández-Rodríguez, T. Rocha-Rinza, Acidity and basicity interplay in amide and imide self-association, Chem. Sci. 9 (19) (2018) 4402–4413.
[53] T. Park, E.M. Todd, S. Nakashima, S.C. Zimmerman, A Quadruply Hydrogen Bonded Heterocomplex Displaying High-Fidelity Recognition, J. Am. Chem. Soc. 127 (51) (2005) 18133–18142.
[54] X. Tang, A. Feula, B.C. Baker, K. Melia, D. Hermida Merino, I.W. Hamley, C. P. Buckley, W. Hayes, C.R. Siviour, A dynamic supramolecular polyurethane network whose mechanical properties are kinetically controlled, Polymer 133 (2017) 143–150.
[55] T.F.A. De Greef, M.M.J. Smulders, M. Wolffs, A.P.H.J. Schenning, R.P. Sijbesma, E. W. Meijer, Supramolecular Polymerization, Chem. Rev. 109 (11) (2009) 5687–5754.
[56] H. Chen, L.R. Hart, W. Hayes, C.R. Siviour, Mechanical characterisation and modelling of a thermoreversible superamolecular polyurethane over a wide range of rates, Polymer 221 (2021) 123607.
[57] K. Zhang, M. Aiba, G.B. Fahs, A.G. Hudson, W.D. Chiang, R.B. Moore, M. Ueda, T. E. Long, Nucleobase-functionalized acrylic ABA triblock copolymers and supramolecular blends, Polym. Chem. 6 (13) (2015) 2434–2444.
[58] K. Zhang, A.M. Nelson, S.J. Talley, M. Chen, E. Margaretta, A.G. Hudson, R. B. Moore, T.E. Long, Non-isocyanate poly(amide-hydroxyurethane)s from sustainable resources, Green Chem. 18 (17) (2016) 4667–4681.
[59] Y. Ji, X. Yang, Z. Ji, L. Zhu, N. Ma, D. Chen, X. Jia, J. Tang, Y. Cao, DFT-Calculated IR Spectrum Amide I, II, and III Band Contributions of N-Methylacetamide Fine Components, ACS Omega 5 (15) (2020) 8572–8578.
[60] S. Sivakova, D.A. Bohnsack, M.E. Mackay, P. Suwanmala, S.J. Rowan, Utilization of a Combination of Weak Hydrogen-Bonding Interactions and Phase Segregation to Yield Highly Thermosensitive Supramolecular Polymers, J. Am. Chem. Soc. 127 (51) (2005) 18202–18211.
[61] R. Sarkar, S. Majumdar, S. Kuil, J. Mallens, J.J.B. van der Tol, R.P. Sijbesma, J.P. A. Heuts, A.R.A. Palmans, Dynamic covalent networks with tunable dynamicity by mixing acylsemicarbazides and thioacylsemicarbazides, J. Polym. Sci. 61 (13) (2023) 1335–1347.
[62] Y. Xu, Z. Xin, S. Yan, C. Yu, J. Liu, Y. Yin, P. Xu, R. Zhou, Z. Sun, Y. Qin, C. Bao, Integrating high mechanical strength, excellent healing ability, and antibacterial ability into supramolecular poly(urethane–urea) elastomers by tailoring the intermolecular supramolecular interactions, Polym. Chem. 14 (25) (2023) 3035–3043.
[63] C. Zhang, Z. Ren, Z. Yin, H. Qian, D. Ma, Amide II and Amide III Bands in Polyurethane Model Soft and Hard Segments, Polym. Bull. 60 (1) (2008) 97–101.
[64] P. Cordier, F. Tournilhac, C. Soulié-Ziakovic, L. Leibler, Self-healing and thermoreversible rubber from supramolecular assembly, Nature 451 (7181) (2008) 977–980.
[65] P.J. Woodward, D. Hermida Merino, B.W. Greenland, I.W. Hamley, Z. Light, A. T. Slark, W. Hayes, Hydrogen Bonded Supramolecular Elastomers: Correlating Hydrogen Bonding Strength with Morphology and Rheology, Macromolecules 43 (5) (2010) 2512–2517.
[66] T. Jing, X. Heng, X. Guifeng, L. Li, P. Li, X. Guo, Rapid self-healing and tough polyurethane based on the synergy of multi-level hydrogen and disulfide bonds for healing propellant microcracks, Mater. Chem. Front. 6 (9) (2022) 1161–1171.
[67] D. Pedrazzoli, I. Manas-Zloczower, Understanding phase separation and morphology in thermoplastic polyurethanes nanocomposites, Polymer 90 (2016) 256–263.
[68] D. Hermida-Merino, L.R. Hart, P.J. Harris, A.T. Slark, I.W. Hamley, W. Hayes, The effect of chiral end groups on the assembly of supramolecular polyurethanes, Polym. Chem. 12 (31) (2021) 4488–4500.
[69] A. Fraix, V. Torrisi, G. Marletta, S. Sortino, P.G. Mineo, G.A. Tomaselli, F. P. Ballistreri, G. Trusso Sfrazzetto, A. Pappalardo, Supramolecular polymer networks based on calix[5]arene chained poly(p-phenyleneethynylene) and C60 fulleropyrrolidine, Supramol. Chem. 28 (5–6) (2016) 485–492.
[70] L. Kan, P. Zhang, H. Jiang, S. Zhang, Z. Liu, X. Zhang, N. Ma, D. Qiu, H. Wei, Microphase separation of a quadruple hydrogen bonding supramolecular polymer: effect of the steric hindrance of the ureido-pyrimidone on their viscoelasticity, RSC Adv. 9 (16) (2019) 8905–8911.
[71] L.-C. Xu, P. Soman, J. Runt, C.A. Siedlecki, Characterization of surface microphase structures of poly(urethane urea) biomaterials by nanoscale indentation with AFM, J. Biomater. Sci. Polym. Ed. 18 (4) (2007) 353–368.
[72] O.J.G.M. Goor, H.M. Keizer, A.L. Bruinen, M.G.J. Schmitz, R.M. Versteegen, H. M. Janssen, R.M.A. Heeren, P.Y.W. Dankers, Efficient Functionalization of Additives at Supramolecular Material Surfaces, Adv. Mater. 29 (5) (2017) 1604652.
[73] J.T. Garrett, C.A. Siedlecki, J. Runt, Microdomain Morphology of Poly(urethane urea) Multiblock Copolymers, Macromolecules 34 (20) (2001) 7066–7070.
[74] J. Zhou, Y. Yang, R. Qin, M. Xu, Y. Sheng, X. Lu, Robust Poly(urethane-amide) Protective Film with Fast Self-Healing at Room Temperature, ACS Appl. Polym. Mater. 2 (2) (2020) 285–294.

[75] Y. Yang, M.W. Urban, Self-healing polymeric materials, Chem. Soc. Rev. 42 (17) (2013) 7446–7467.
[76] G.L. Wilkes, R. Wildnauer, Kinetic behavior of the thermal and mechanical properties of segmented urethanes, J. Appl. Phys. 46 (10) (2008) 4148–4152.
[77] C.-C. Cheng, F.-C. Chang, J.-K. Chen, T.-Y. Wang, D.-J. Lee, High-efficiency self-healing materials based on supramolecular polymer networks, RSC Adv. 5 (122) (2015) 101148–101154.
[78] W. Fan, Y. Jin, L. Shi, W. Du, R. Zhou, Transparent, eco-friendly, super-tough "living" supramolecular polymers with fast room-temperature self-healability and reprocessability under visible light, Polymer 190 (2020) 122199.
[79] J.H. Yang, J. Lee, S. Lim, S. Jung, S.H. Jang, S.-H. Jang, S.-Y. Kwak, S. Ahn, Y. C. Jung, R.D. Priestley, J.W. Chung, Understanding and controlling the self-healing behavior of 2-ureido-4[1H]-pyrimidinone-functionalized clustery and dendritic dual dynamic supramolecular network, Polymer 172 (2019) 13–26.
[80] Q. Zhang, C.-Y. Shi, D.-H. Qu, Y.-T. Long, B.L. Feringa, H. Tian, Exploring a naturally tailored small molecule for stretchable, self-healing, and adhesive supramolecular polymers, Science, Advances 4 (7) (2018) eaat8192.
[81] Y. Yu, S. Wang, L. Jia, M. Zhou, Q. Pan, Y. Zhai, C. Wang, Organogels from different self-assembling novel l-proline dihydrazide derivatives: gelation mechanism and morphology investigations, JSST 78 (1) (2016) 218–227.
[82] Z. Zhang, H. Mei, Q. Wang, R. Li, G. Wang, H. Wei, X. Ouyang, Self-healing polyurethane elastomer based on 2-ureido-4[1H]-pyrimidinone, Mater. Chem. Phys. 285 (2022) 126070.
[83] J. Liu, X. Ma, Y. Tong, M. Lang, Self-healing polyurethane based on ditelluride bonds, Appl. Surf. Sci. 455 (2018) 318–325.
[84] X. Jin, N. Guo, Z. You, Y. Tan, Design and Performance of Polyurethane Elastomers Composed with Different Soft Segments, Materials (basel) 13 (21) (2020).
[85] X. Yan, Z. Liu, Q. Zhang, J. Lopez, H. Wang, H.-C. Wu, S. Niu, H. Yan, S. Wang, T. Lei, J. Li, D. Qi, P. Huang, J. Huang, Y. Zhang, Y. Wang, G. Li, J.B.H. Tok, X. Chen, Z. Bao, Quadruple H-Bonding Cross-Linked Supramolecular Polymeric Materials as Substrates for Stretchable, Antitearing, and Self-Healable Thin Film Electrodes, J. Am. Chem. Soc. 140 (15) (2018) 5280–5289.
[86] M. Liu, Z. Wang, P. Liu, Z. Wang, H. Yao, X. Yao, Supramolecular silicone coating capable of strong substrate bonding, readily damage healing, and easy oil sliding, Science, Advances 5 (11) (2019) eaaw5643.
[87] Y. Deng, Q. Zhang, C. Shi, R. Toyoda, D.-H. Qu, H. Tian, B.L. Feringa, Acylhydrazine-based reticular hydrogen bonds enable robust, tough, and dynamic supramolecular materials, Sci. Adv. 8 (4) (2022) eabk3286.